ELSEVIER

Physica B 226 (1996) 331–337

PHYSICA B

Temperature dependence of optical phonon lifetimes in ZnSe

Suruchi Anand, Prabhat Verma*, K.P. Jain, S.C. Abbi

Department of Physics, Indian Institute of Technology, Hauz Khas, New Delhi 110016, India

Received 10 May 1996

Abstract

Temperature-dependent Raman scattering experiments were performed on the ⟨1 1 1⟩ face of crystalline ZnSe to estimate the phonon lifetimes for the LO and TO phonons for temperatures between 20 and 300 K. The lifetimes at higher temperatures are mainly due to the anharmonic decay of optical phonons into low-energy phonons. The temperature-independent contributions from inherent crystal defects and from boundary scattering become comparable to the phonon scattering contribution at lower temperatures. The temperature dependence of the population of the acoustic mode (2TA) is found to follow Bose–Einstein statistics.

1. Introduction

The II–VI wide band gap semiconductors have been extensively studied in the literature [1–6], little attention has been paid to the propagation of phonons and their relaxation times. An in-depth understanding of the phonon propagation is of great technological importance, especially for systems such as ZnSe, which are finding increasing applications, not only in fast electronic devices, but also in blue semiconductor lasers and other optoelectronic devices.

The photon lifetimes as a function of temperature can be accurately measured by Raman spectroscopy. The lifetimes of optical phonons in ZnSe have been estimated [5] at 5 and 100 K in the past using time-resolved coherent anti-Stoke's Raman scattering (TRCARS). However, the temperature-dependent Raman scattering measurement can be used to estimate not only the temperature variation of the phonon lifetimes, but also the anharmonicity in the vibrational potential accurately [6]. It is well-known [7,8] that the phonon relaxation rates are frequently dominated by the decay of strongly interacting optical phonons into weakly interacting low-energy phonons. The finite values of the lifetimes are predominantly due to phonon–phonon interaction, which is highly temperature-dependent, but also has a contribution due to the scattering by crystal defects, and boundary scattering (phonon propagation is limited by the sample dimension) which is almost temperature-independent [9].

In this paper, we present a detailed temperature-dependent Raman study of crystalline ZnSe with particular reference to the zone centre one-phonon TO and LO modes and the zone edge two-phonon acoustic mode in the temperature range between 20 and 300 K. The aim of this work is, firstly, to

*Corresponding author.

PII S0921-4526(96)00046 6-8

ascertain the phonon lifetimes for the TO and LO phonons due to anharmonic decay. The anharmonicity present in the vibrational potential for the two modes is estimated by means of numerically calculating the anharmonic constants. Furthermore, the temperature-independent broadening due to the inherent disordered nature of the crystal and boundary scattering is also estimated for the two modes. It is found that the effect of disorder is greater for the TO phonon than for the LO phonon. A similar result was previously observed by Bairamov et al. [9] for GaP. Secondly, we present the results of the temperature-dependent Raman study of the 2TA phonon mode at the X-point of the Brillouin zone. The propagation of an acoustic phonon is different from that of an optical phonon. The momentum conservation does not allow anharmonic decay of the acoustic phonon. No appreciable temperature-dependent change in the position and the width of the 2TA mode was observed. However, the intensity of this structure is found to be very sensitive to the lattice temperature. A similar result was earlier [10] seen for GaAs, where the temperature dependence was explained in terms of Bose–Einstein statistics.

2. Experimental procedure

The Raman scattering experiments were performed in the back-scattering geometry by employing the 514.5 nm wavelength of an argon-ion laser, the Ramanor double monochromator and usual photon counting electronics. The $\langle 1\,1\,1\rangle$ face of a 500 μm-thick bulk ZnSe sample was fixed on the cold finger of a cryostat using silver paste, and the temperature was regulated down to 20 K from room temperature using the Helitron closed cycle liquid-He cryostat. The cryostat was evacuated to 1×10^{-6} Torr to avoid condensation of moisture on the sample at low temperatures. The monochromator was calibrated using strong plasma lines of the argon-ion laser and for better accuracy, the slit width of the monochromator was reduced to 75 μm. For this slit width, the instrumental error is less than 0.5 cm^{-1}, which is calculated from the geometry of the optics. The temperature of the sample was measured accurately by mounting a thermocouple on the cold finger. Each spectrum was recorded three times and the average values of line widths and line centres were taken. The instrumental line profile function was also deconvoluted from the experimental values to obtain the true intrinsic phonon frequencies and widths. This process is discussed elsewhere [10]. The Raman experiments were performed at seven different temperatures between 20 and 300 K.

3. Experimental results and discussion

3.1. The optical phonons

The line centres and the line widths of optical phonons (LO and TO) are found to vary with temperature. These temperature-dependent changes can be attributed to the anharmonicity in the vibrational potential, which leads to the decay of optical phonons into low-energy phonons. An optical phonon can in general decay into two phonons (three-phonon process), three phonons (four-phonon process) or more phonons. These decays are such that energy and momentum conservation are obeyed. The probability of higher-order processes rapidly decreases, and at temperatures below the Debye temperature of the sample, only the three-phonon process [10,13] is dominant. In this case, the two final phonons can have frequencies ω' and $(\omega_0-\omega')$, and wave vectors $\boldsymbol{q}$ and $-\boldsymbol{q}$, respectively, where ω_0 is the optical phonon frequency. For a given optical phonon, one can find a combination of two low-energy phonons which can satisfy both energy and momentum conservation. From the phonon dispersion curve for ZnSe, we have estimated the following decay channels which satisfy the conservation laws:

$\mathrm{LO}(\omega_0)\rightarrow$ (a) $\mathrm{LA}(\omega_0/2)+\mathrm{LA}(\omega_0/2)$ in the $\langle 1\,0\,0\rangle$ direction

(b) $\mathrm{LA}(49\ cm^{-1})+\mathrm{TO}(209\ cm^{-1})$ in the $\langle 1\,0\,0\rangle$ direction

(c) LA(182 cm^{-1}) + TA(76 cm^{-1}) in the $\langle 1\,0\,0\rangle$ direction
(d) LA(158 cm^{-1}) + TA(100 cm^{-1}) in the $\langle 1\,1\,0\rangle$ direction

TO(ω_0) → (a) LA($\omega_0/2$) + LA($\omega_0/2$) in the $\langle 1\,0\,0\rangle$ direction
(b) LA(140 cm^{-1}) + TA(71 cm^{-1}) in the $\langle 1\,0\,0\rangle$ direction
(c) LA(127 cm^{-1}) + TA(84 cm^{-1}) in the $\langle 1\,1\,0\rangle$ direction

Furthermore, the inherent disorder in the crystal provides decay channels and leads to broadening of the phonon. This term is almost temperature-independent. The present work is carried out below the ambient temperature which is below the Debye temperature of ZnSe (450 K), thus the three-phonon process is dominant and the higher order decay processes can be neglected. This problem has generally been considered [10–13] as one optical phonon decaying into two acoustic phonons of same frequency and opposite momenta (the decay process labelled (a) above). Considering only the three-phonon process, the temperature variation of the phonon line width and line centre have been given by various authors [9–10] as

$$\Gamma(T) = \Gamma_0 + A\left\{1 + \frac{2}{e^{\hbar(\omega_0/2)/k_B T} - 1}\right\}, \tag{1}$$

and

$$\omega(T) = \omega_0 + C\left\{1 + \frac{2}{e^{\hbar(\omega_0/2)/k_B T} - 1}\right\}, \tag{2}$$

where ω_0 is the intrinsic frequency of the optical phonon and $\omega_0/2$ is the frequency of the acoustic phonons, Γ_0 is the broadening due to the disorder in the crystal and the constants A and C are the anharmonic constants.

Other possible decay channels have been neglected by these authors. However, Menendez et al. [6] and Bron et al. [14] have discussed the possibilities of other channels. Considering all the possible decay channels, Eqs. (1) and (2) can be rewritten as

$$\Gamma(T) = \Gamma_0 + A\left\{1 + \frac{1}{e^{\hbar(\omega')/k_B T} - 1} + \frac{1}{e^{\hbar(\omega_0 - \omega')/k_B T} - 1}\right\}, \tag{3}$$

$$\omega(T) = \omega_0 + C\left\{1 + \frac{1}{e^{\hbar(\omega')/k_B T} - 1} + \frac{1}{e^{\hbar(\omega_0 - \omega')/k_B T} - 1}\right\}, \tag{4}$$

where ω' and $(\omega_0 - \omega')$ are the frequencies of the two final phonons, respectively. The present signal-to-noise ratio of the experimental data prevents a clear cut differentiation between the various decay channels. The calculations of the joint density-of-states for phonons can give the dominant decay process out of all possible channels. We do not have this calculation, and so we consider all possible decay channels independently.

The TO and LO phonons in the room temperature Raman spectrum typically appear at 205.5 and 251.5 cm^{-1}, respectively. Fig. 1 shows the TO and the LO phonon in the Raman spectra of ZnSe at various temperatures between 20 and 300 K. The average deconvoluted experimental values of the line width and line centre for the one-phonon TO and LO modes in the Raman spectrum of crystalline ZnSe for these temperatures are plotted in Figs. 2 and 3, respectively. Eqs. (3) and (4) have been used to fit these experimental Figs. 2 and 3, respectively. Eqs. (3) and (4) have been used to fit these experimental data by suitably choosing the constants ω_0, Γ_0, A and C. Various curves in Figs. 2 and 3 show the best fit for different possible decay channels. The value for these constants for the TO and LO phonons are given in Table 1. Figs. 2 and 3 show good agreement between the calculated curves, given by the various lines, and the experimental values shown by circles and crosses.

Figs. 2 and 3 typically show that the line width increases whereas the line centre shifts downwards with increasing temperature. The thermal interaction is large at higher temperatures which decreases the phonon mean free path, and so the decay lifetime decreases as the temperature of the system is

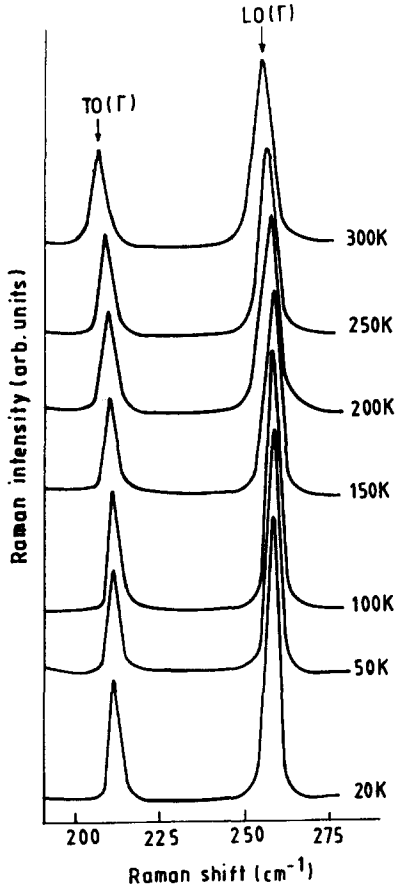

Fig. 1. Raman spectra of the ⟨1 1 1⟩ face of ZnSe at various temperatures showing the one-phonon optical modes.

increased. This leads to the increased line width at higher temperatures. Assuming the true phonon line shape to be Lorentzian, we can use the simple relation [15]

$$\tau = \frac{1}{\pi c \Gamma} \tag{5}$$

to estimate the relaxation time for the decay process, where c is the velocity of light and Γ is the line width. The estimated values of lifetimes for the decay processes are given in Table 2. Table 2 also gives the reported values of the relaxation times estimated by TRCARS [5]. The published results [5] do not discuss the relaxation times for the TO phonon. However, our results are in good

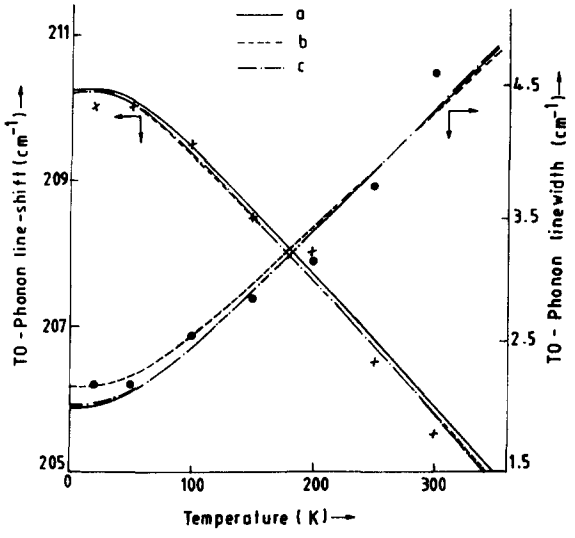

Fig. 2. Temperature variation in the line centre and line width for the one-phonon TO mode for ZnSe. The solid curves give theoretical fits using Eqs. (3) and (4), and the experimental points are shown by circles and crosses. The curves labelled (a)–(c) correspond to the decay processes labelled (a)–(c) in the text.

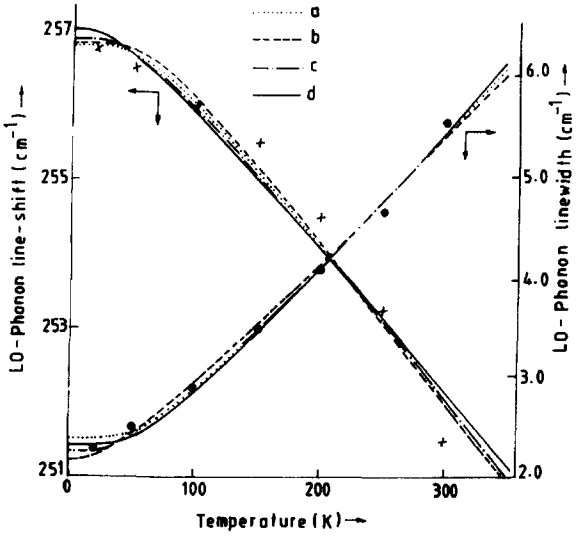

Fig. 3. Temperature variation in the line centre and line width for the one-phonon LO mode for ZnSe. The solid lines give theoretical fits using Eqs. (3) and (4), and the experimental points are shown by circles and crosses. The curves labelled (a)–(d) correspond to the decay processes labelled (a)–(d) in the text.

Table 1
The values of various constants involved in Eqs. (3) and (4) for the best theoretical fit to the experimental results for the TO and LO phonons

Phonon mode	Decay channel	ω_0 (cm^{-1})	ω' (cm^{-1})	$\omega_0 - \omega'$ (cm^{-1})	Γ_0 (cm^{-1})	A (cm^{-1})	C (cm^{-1})
LO	(a)	258.9	129.5	129.5	1.027	1.353	−2.077
	(b)	258.1	49.0	209.0	1.415	0.758	−1.125
	(c)	258.5	182.0	76.0	1.162	1.093	−1.637
	(d)	258.7	158.0	100.0	1.014	1.293	−1.943
TO	(a)	211.7	105.8	105.8	1.444	0.738	−1.451
	(b)	211.5	140.0	71.0	1.322	0.693	−1.291
	(c)	211.6	127.0	84.0	1.278	0.755	−1.407

Table 2
Estimated lifetimes for the anharmonic decay of LO and TO phonons in ZnSe

Phonon mode	Temperature (K)	Lifetime (ps)
LO	300	1.89 ± 0.1
	100	3.66 ± 0.6
		3.60 ± 0.3[a]
	20	4.61 ± 1.0
	5	4.70 ± 0.3[a]
TO	300	2.26 ± 0.2
	100	4.08 ± 0.8
	20	4.61 ± 1.0

[a]Ref. [5].

agreement with their values for the LO phonon. Fig. 4 shows the temperature dependence of the phonon lifetime for the two phonons. The solid lines in Fig. 4 are theoretical fits for the decay processes labelled (a), using Eqs. (3) and (5), the solid circles show our experimental values and the hollow circles in Fig. 4(a) give the LO phonon lifetime calculated by Kuhl et al. [5].

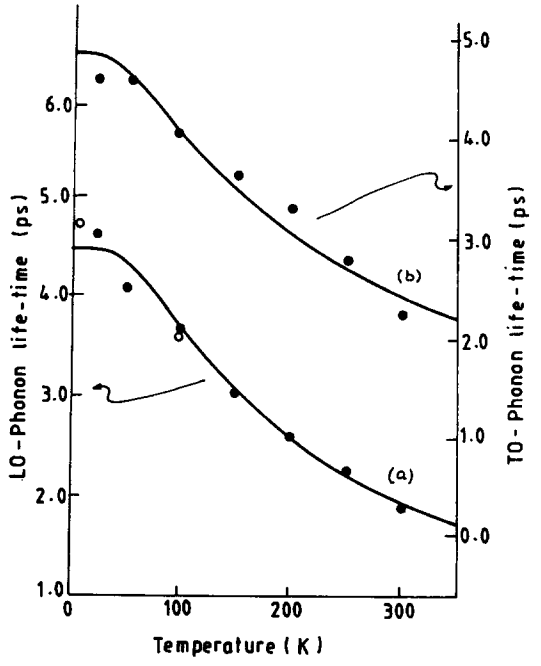

Fig. 4. Temperature variation in the phonon lifetime for (a) LO and (b) TO phonons. The solid curves show theoretical fits for the decay labelled (a) in the text, and the solid circles show our experimental results. The hollow circles are the values taken from Ref. [5].

3.2. The acoustic phonon

The one-phonon acoustic modes are symmetry forbidden. The two-phonon transverse acoustic (2TA) modes are observed between 80 and 200 cm^{-1} in the Raman spectrum of ZnSe. The dominant structure is due to the 2TA mode at the X-point of the Brillouin zone, which gives a peak at about 140.5 cm^{-1}. The acoustic phonons do not show anharmonic effects, mainly because the momentum conservation does not allow their anharmonic decay. Thus, no appreciable temperature-dependent changes are observed in the line centre and the line width for the 2TA structure. Fig. 5

gives the 2TA structure for crystalline ZnSe at various temperatures. It can be seen from Fig. 5 that the intensity of the structure rapidly decreases with temperature. With the $\lambda = 514.5$ nm wavelength of the Ar^+ laser, we are far away from the band gap, avoiding any resonance effect. A similar change was observed [10] for GaAs earlier, and was discussed in terms of Bose–Einstein statistics.

For a broad structure, such as in Fig. 5, the area under the mode structure is proportional to the number of phonons taking part in the scattering process. Due to the ceration and annihilation of phonons at any finite temperature, the total number of phonons participating in the scattering process is proportional to their occupation number. In terms of the Bose–Einstein function $n_B = 1/(e^{\hbar\omega_0/k_BT} - 1)$, the occupation number can be written as $n = 1 + n_B$.

The experimental values of the area under mode structure (in arbitrary units) at various temperatures are given in Table 3, for the 2TA mode in crystalline ZnSe. Also given in Table 3 are the normalized values A_n of the areas, calculated by changing the scale and shifting the origin ($A_n = P \cdot A + Q$, where P and Q are constants and A is the area under mode structure). This normalization does not change the basic behaviour of the

Table 3
The area under mode structure and the normalized values of areas under mode structures for the 2TA mode in the Raman spectra of ZnSe

Temperature (K)	Area under mode-structure (arb. units)	Normalized area (arb. units)
20	850	1.19
50	850	1.19
100	1262	1.71
150	1500	2.01
200	1675	2.23
250	2375	3.11
300	2600	3.40

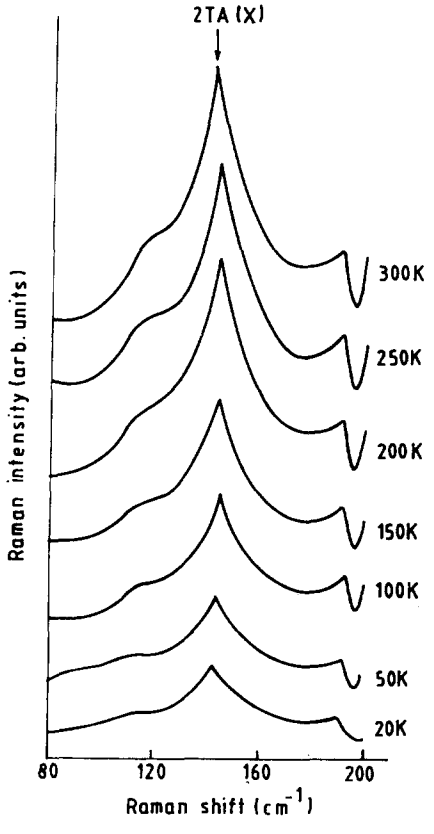

Fig. 5. Raman spectra showing the 2TA mode for ZnSe at various temperatures.

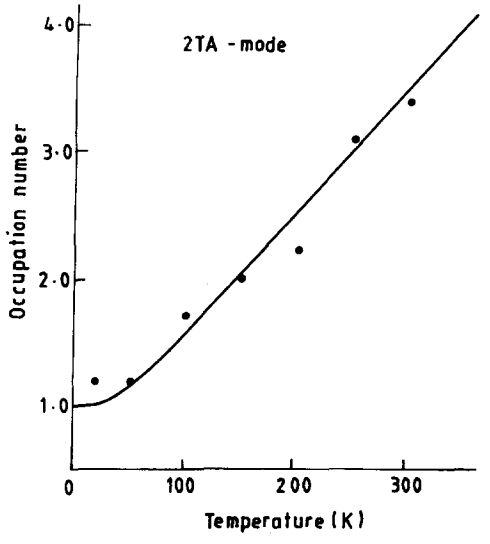

Fig. 6. Temperature variation in the area under mode structure for the 2TA mode. The solid line gives theoretical fit obtained from the occupation number and the circles show the experimental values of normalized area.

temperature dependence. The normalization was properly done so that the normalized area can be compared with the theoretical value of the occupation number n. The solid curve in Fig. 6 shows the temperature dependence of the occupation number n for $\omega_0 = 140.5\ \mathrm{cm}^{-1}$, and the circles are the normalized values of the areas under the mode structure at various temperatures as given in Table 3. This figure shows a good agreement between the theoretical values of the occupation number and the normalized experimental values of the area under mode structure.

4. Conclusions

The temperature-dependent Raman scattering indicates that the decrease in the phonon lifetime with increasing temperature is predominantly due to the decay of strongly interacting optical phonons into weakly interacting low-energy phonons. A contribution for the phonon lifetime also comes from the scattering by inherent crystal defects and from the boundary scattering, but this contribution is found to be temperature-independent. The lifetime for the decay of the LO phonon in ZnSe varies from about 1.89 ps at room temperature to about 4.61 ps at 20 K, whereas for the TO phonon, it varies from about 2.26 ps at room temperature to about 4.61 ps at 20 K.

The anharmonic effects are found to be absent for the acoustic mode (2TA). The rapid temperature-dependent change in the oscillator strength of the acoustic mode matches well with the temperature variation in the occupation number.

Acknowledgements

This work was sponsored by the Department of Science and Technology, Government of India, under the research project entitled Laser Raman and Photoluminescence Spectroscopy of II-VI Wide Band gap Semiconductors.

References

[1] H.H. Li, J. Phys. Chem. Ref. Data 13 (1984) 103.
[2] L. Ward, in: Handbook of Optical Constants of Solid II, ed. E. Palik (Academic Press, New York, 1991) pp. 737–758.
[3] E.A. Vinogradov, G.N. Zhizhin, A.G. Malshukov and V.I. Yudson, Solid State Commun. 23 (1977) 915.
[4] V.M. Burlakov, E.A. Vinogradov, G.N. Zhizhin and V.I. Rupasov, Sov. Phys. Solid State 22 (1980) 57.
[5] J. Kuhl, B.K. Rhee and W.E. Bron, Phonon Scattering in Condensed Matter, Proc. IVth Int. Conf., Stuttgart, Germany (1983) pp. 106–108.
[6] J. Menendez and M. Cardona, Phys. Rev. B 29 (1984) 2051.
[7] S. Das Sarma, in: Hot Carriers in Semiconductor Nanostructures: Physics and Applications, ed. J. Shah (Academic Press, Boston, 1992) pp. 53–85.
[8] S. Das Sarma, V.B. Compos, M.A. Stroscio and K.W. Kim, Semicond. Sci. Tehnol. 7 (1992) B60.
[9] B.K. Bairamov, Y.E. Kitaev, V.K. Negoduika and Z.M. Khashkhozhev, Sov. Phys. Solid State 16 (1975) 1323.
[10] Prabhat Verma, S.C. Abbi and K.P. Jain, Phys. Rev. B 51 (1995) 16660.
[11] P.G. Klemens, Phys. Rev. 148 (1966) 845.
[12] T.R. Hart, R.L. Aggarwal and Benjamin Lax, Phys. Rev. B 1 (1970) 638.
[13] M. Balkanski, R.F. Wallis and E. Haro, Phys. Rev. B 28 (1983) 1928.
[14] W.E. Bron, J. Kuhl and B.K. Rhee, Phys. Rev. B 34 (1986) 6961.
[15] See, for example, O. Svelto and D.C. Hanna, Principles of Lasers (Plenum Press, New York, 1982) p. 52.